



# CHORUS

This is the accepted manuscript made available via CHORUS. The article has been published as:

## Nuclear Scission and Quantum Localization

W. Younes and D. Gogny

Phys. Rev. Lett. **107**, 132501 — Published 21 September 2011

DOI: [10.1103/PhysRevLett.107.132501](https://doi.org/10.1103/PhysRevLett.107.132501)

# Nuclear Scission and Quantum Localization

W. Younes and D. Gogny

*Lawrence Livermore National Laboratory, Livermore, CA 94551*

We examine nuclear scission within a fully quantum-mechanical microscopic framework, focusing on the non-local aspects of the theory. Using  $^{240}\text{Pu}$  hot fission as an example, we discuss the identification of the fragments and the calculation of their kinetic, excitation, and interaction energies, through the localization of the orbital wave functions. We show that the “disentanglement” of the fragment wave functions is essential to the quantum-mechanical definition of scission and the calculation of physical observables. Finally, we discuss the fragments’ pre-scission excitation mechanisms and give a non-adiabatic description of their evolution beyond scission.

PACS numbers: 24.75.+i,21.60.Jz,25.85.-w

Nuclear scission, the process wherein a nucleus breaks into two or more fragments, poses a fundamental challenge to quantum many-body theory: scission implies a separation of the nucleus into independent fragments, while the Pauli exclusion principle introduces a persistent correlation between the fragments, no matter how far apart they are. The objective of this paper is to resolve this paradox by disentangling the fragments in a fully quantum-mechanical description that is consistent with experimental data. In addition to shedding light on fundamental aspects of many-body physics, a microscopic theory of scission is needed to make reliable predictions of fission-fragment properties, such as their excitation and kinetic energies, and their shapes. In particular, we revisit in a microscopic approach the question of the energy partition between light and heavy fragments which was addressed in a recent letter [1] within a statistical-mechanic treatment. While many technical challenges remain in the 70-year quest to develop a predictive theory of fission, understanding scission, remains a formidable conceptual obstacle to such a theory.

Previous descriptions of scission have always been formulated within the context of a local nuclear density, with an identifiable neck joining two pre-fragments. The neck ruptures at some point along its length, and all the matter to one side or the other of the rupture is relegated to the corresponding fragment. Despite its usefulness, this is ultimately a classical view of scission. In 1959 [2], this picture was used to qualitatively account for the different observed mass divisions in fission and the well-known “sawtooth” shape of the average neutron-multiplicity distribution. Later on, a more quantitative description of the nuclear shape was introduced [3], and scission was equated with a vanishing neck size. This criterion was later improved [4] by requiring that scission occurs when the Coulomb repulsion exceeds the attractive nuclear force between the fragments. Nörenberg [5] took a step toward a more microscopic description using a molecular model of fission calculated in a two-center Hartree-Fock+BCS approach. Bonneau *et al.* [6] used separate microscopic calculations of each fragment and a phenomenological nuclear interaction between them to define a scission criterion based on the ratio of their mutual nuclear and Coulomb energies. In recent calculations [7, 8, 10] the entire fissioning nucleus was treated within a single microscopic framework and the properties of the nucleus at scission were calculated. In those calculations however, the identification of scission and calculations of fragment properties still relied on the nuclear density. In contrast to previous approaches, we present here a fully quantum-mechanical description of scission that accounts for the nonlocality of the many-body wave function of the nucleus. The need for, and difficulty of disentangling the fragment wave functions was alluded to in [6]. Our solution is in the spirit of the Localized Molecular Orbital (LMO) technique used in molecular physics [9]: as explained below, we extend the LMO concept to localize individual quasiparticle orbitals on the fragments while the nucleons themselves, described by a Bogoliubov vacuum built from these states, remain delocalized. In this way, we are able to recognize the fragments and their interaction energy progressively, as we approach scission. This powerful technique has never been used to describe nuclear scission before.

The work described in this paper is based on constrained Hartree-Fock-Bogoliubov (HFB) calculations of  $^{240}\text{Pu}$  with a finite-range (D1S) interaction. Details of the calculation are given in [10]. We have chosen to focus on the hot-scission point with constrained quadrupole moment  $Q_{20} = 370$  b [17], and used the constraint on neck size,  $Q_N$ , to approach scission. This constraint, defined in [10], lets us vary the number of particles in the neck region. HFB calculations produce self-consistent solutions that minimize the total energy of the nucleus. In order to describe the nucleus near scission, we introduce here the additional requirement that the interaction energy between pre-fragments must be minimized. This criterion is consistent with the physical picture of the pre-fragments evolving into independent fragments that move increasingly further apart. We have shown in previous work [10, 11] that the pre-fragments in the HFB solutions near scission generally exhibit “tails”, portions of contributions to the total density from individual quasiparticles (qp) that extend into the complementary fragment. Our calculations show that the size of these tails is closely related to the strength of the interaction between the fragments. Therefore, minimization of the interaction

energy between fragments is essentially equivalent to localization of the qp orbitals on the fragments.

Hartree-Fock methods in molecular (or nuclear) physics generally produce single-particle atomic orbitals that are not spatially localized within a molecule (nucleus). However, it was observed early on [9] that any unitary transformation applied to the single-particle components of a Slater determinant does not affect the global properties of the corresponding system. Since then, unitary transformations have been routinely used to localize electron orbitals and thereby define such chemically meaningful concepts as core and bond orbitals. In nuclear fission, we will extend the concept to localize nuclear qp states on the nascent fragments, taking advantage of the fact that the Bogoliubov vacuum is only defined up to a unitary transformation of the qp destruction operators. More precisely, for each qp  $i$ , we calculate its contribution  $\rho_i(\vec{r})$  to the total density. Integration of  $\rho_i(\vec{r})$  with respect to  $\vec{r}$  defines an occupation probability  $v_i^2$  of the qp. We introduce occupations  $(v_i^L)^2$  and  $(v_i^R)^2$  resulting from the integration of  $\rho_i(\vec{r})$  to the left and right of the neck position, respectively. We can then define a localization parameter  $\ell_i \equiv \left| (v_i^L)^2 - (v_i^R)^2 \right| / v_i^2$  for each qp. A value  $\ell_i = 0$ , for example, corresponds to a completely delocalized qp. Our goal then is to maximize the  $\ell_i$  (or equivalently, minimize the tails) by mixing pairs of qp together. Thus, pairs  $(i, j)$  of qp are mixed by an orthogonal transformation with angle  $\theta_{ij}$  chosen to maximize the quantity  $v_i^2(\theta_{ij})\ell_i^2(\theta_{ij}) + v_j^2(\theta_{ij})\ell_j^2(\theta_{ij})$ . Through a systematic search algorithm, a set of qp pairs and their mixing angles is therefore found that minimizes the summed tail size of the two fragments. In selecting these pairs, we have required that the level energies of the qp pairs are no more than 2 MeV apart (the localization procedure is most effective for states that are close in energy). The interest of this process is that, as the neck decreases, one can identify pre-fragments built from qps that are spatially localized. In particular, the density matrix  $\hat{\rho}$  (and pairing tensor  $\hat{\kappa}$ ) can be decomposed as a sum of predominantly left ( $\hat{\rho}^L$ ) and right ( $\hat{\rho}^R$ ) terms. Of course, high-energy (continuum) orbitals can never be well localized, but their occupations are very small and therefore they do not contribute significantly to expectation values of operators. The interaction energy between fragments can now be identified as the contribution to the total energy from cross terms,  $\hat{\rho}^L$  with  $\hat{\rho}^R$  (and  $\hat{\kappa}^L$  with  $\hat{\kappa}^R$  for pairing). The nuclear component of that interaction energy (i.e., excluding the direct Coulomb repulsion between fragments) is plotted in Fig. 1 before and after tail reduction. In both cases individual qps are assigned to one fragment or the other based on their spatial localization relative to the neck position. The effect of the tail reduction can be rather substantial even when the neck between the fragments is small, e.g. by  $\sim 20$  MeV even when  $Q_N < 0.5$ .

We show in Fig. 2 more details concerning the localization of the qps with occupation  $v^2$  according to whether they are preferentially holes ( $v^2 > 1/2$ ) or particles ( $v^2 < 1/2$ ). We observe that the effect of the localization is most visible for the hole states with  $v^2 > 0.7$ . Note in particular the pair of deeply-bound states in the top panel of Fig. 2 with  $v^2 \approx 1$  and  $\ell \approx 0$  (i.e., fully delocalized), both with K quantum number 1/2 and only 7 keV apart in energy. These two states become fully localized in the bottom panel. Notice also that a great number of well-localized qps of particle type can combine with well-localized qps of hole type to provide a rich spectrum of two-qp states, themselves well localized on each of the two pre-fragments. These simple excitations or combinations of them describe excited fragments. We were able to construct such 2-qp excitations of up to 20 MeV, localized on the fragments. Not all states are fully localized by the algorithm above, in particular a 2-MeV, K = 1/2 neutron state remains in the bottom panel with  $v^2 \approx 0.16$  and  $\ell \approx 0.53$  (which means that  $\approx 25\%$  of that qp's occupation probability is in its tail), but the overall effect on the fragment densities shown in the inset in Fig. 1 is significant. The effect of the localization on the interaction energy is even more striking, as shown in Fig. 1. We point out that this analysis includes  $\approx 1100$  proton and neutron qp states.

If we faithfully apply the variational principle to the fissioning nucleus in order to minimize the total energy (by the HFB method), the result will be two infinitely separated fragments in their respective ground states. Experimental observables—neutron emission and kinetic energies—clearly indicate that we must depart from this adiabatic picture. In fact, the point where the evolution of the fissioning nucleus ceases to be adiabatic could be taken as a definition of scission. For practical applications, we give the following 3 criteria that define the scission point: 1) the repulsive Coulomb force between fragments greatly exceeds their mutual nuclear attraction, 2) the exchange contribution to the interaction between fragments is small, which means that we can neglect the antisymmetry between their constituents and describe the system as two separate Bogoliubov vacua beyond the scission point, and 3) in each fragment, we can excite a set of two-qp states that remain localized on the fragments, so that the fragments can be considered as separate entities with their own excitations and in interaction through a repulsive force acting only on their respective centers of mass. As the neck is reduced in our  $^{240}\text{Pu}$  calculation, the point at  $Q_N = 0.35$  is the first for which all three criteria above are simultaneously verified, and the results in Figs. 2 and 1 (inset) were calculated for this scission point. Scission may occur at other nearby points, but this one is representative. At  $Q_N = 0.35$ , the Coulomb force is

$\approx 30$  times larger than the nuclear one, the two-body exchange contribution is only -0.7 MeV (Fig. 1), and a set of 2-qp states can be constructed from localized states in Fig. 2 that remain localized within a fragment. The pairing tensor  $\kappa$  is non-local and provides an additional test of the localization of the fragments. We find that the correspond pairing energy is also only -0.7 MeV between fragments at scission out of -20 MeV for the entire nucleus. Thus, for the first time in the literature, we give a definition of scission that does not ignore the non-local aspects of quantum mechanics.

This leads us to describe our system after scission in the Hill-Wheeler approximation as  $\Psi = \int f(d) \Phi_d dd$  where  $d$  is the relative distance between the fragments, and  $\Phi_d \equiv \Phi_1 \Phi_2$  is the two fragments' wave function. We obtain the collective Hamiltonian [12],

$$H_{\text{coll}} \equiv \frac{\vec{p}_d^2}{2\mu m} + V(d) + C$$

where  $\vec{p}_d$  is the momentum operator corresponding to  $d$ ,  $\mu$  is the reduced mass of the fragments with masses  $A_1$  and  $A_2$ , and  $m$  is the nucleon mass,  $V(d)$  is the fragment interaction potential, and  $C = E_i + \varepsilon_0$  is a constant, with  $E_i$  ( $i = 1, 2$ ) the internal fragment energy, and  $\varepsilon_0$  a zero-point correction,

$$E_i \equiv \left\langle \Phi_i \left| H - \frac{\vec{p}_i^2}{2mA_i} \right| \Phi_i \right\rangle$$

$$\varepsilon_0 \equiv \left\langle \Phi_d \left| \frac{\vec{p}_1^2}{2mA_1} + \frac{\vec{p}_2^2}{2mA_2} - \frac{\vec{p}^2}{2mA} \right| \Phi_d \right\rangle$$

Note that  $V(d_s) + C$  is nothing but the total Bogoliubov energy at the scission point (i.e., at  $d = d_s$ ). The form of  $\varepsilon_0$  is due to the fact that we subtract the center of mass energy,  $\vec{p}^2/2mA$ , of the mass- $A$  fissioning nucleus throughout the fission process.

Thus we propose the following two-stage description of fission: 1) the nucleus deforms until it reaches a scission configuration determined with the criteria given above at which point the fragments are “frozen” in their configurations and 2) as a result of their strong mutual repulsion move apart essentially by spatial translation. Eventually these fragments will decay by neutron and gamma emission to their respective ground states. This is essentially a picture of fission in the sudden approximation. Note that all approaches that study the scission point depend on simplifying approximations (e.g., sudden approximation in the liquid-drop model [4]) or strong hypotheses (e.g., thermal equilibrium [1]).

This microscopic picture of scission can be readily integrated into the larger context of the time-dependent generator-coordinate method (TDGCM). For example, in a two-dimensional description in terms of the  $Q_{20}$  and  $Q_{30}$  moments of the nucleus, we identify a set of points in this  $Q_{20} - Q_{30}$  space that define a boundary between an internal region (pre-scission) and an external region (post-scission) using the scission criteria above [10]. The Hill-Wheeler equation constructed in the internal region then allows us to follow a wave packet from the first well to this boundary [7], and therefore to deduce the probability of populating different scission configurations.

In the following we investigate the extent to which this picture is consistent with experimental observables. Let us first discuss our predictions assuming a one-dimensional path leading to the hot fission point and that the collective dynamic is adiabatic from the saddle to the scission point. Starting with zero energy at the saddle we are at  $\approx 25$  MeV above the scission point. With our assumption this energy must be interpreted as a collective pre-kinetic energy. Now, the kinetic energy acquired by the fragments after scission is simply given by  $V(d_s) - V(\infty) = V(d_s)$  which is  $\approx 170$  MeV according to our calculations. Adding this pre-kinetic energy, our description gives a total kinetic energy (TKE) of 195 MeV which exceeds by only 10 MeV the experimental value  $184.8 \pm 1.7$  MeV obtained by averaging the data sets available in the literature [13–15].

The calculation of the fragment excitation energies requires their corresponding ground-state energies, obtained by HFB calculations without the constraint on neck size. Excitation energies of 4.5 MeV and 7 MeV were obtained for the heavy (average mass number  $\approx 132$ ) and light (average mass number  $\approx 108$ ) fragment, respectively. Together, these yield a total excitation energy (TXE) of  $\approx 11.5$  MeV. By contrast, the average TXE expected from empirical arguments [16] in thermal fission on a  $^{239}\text{Pu}$  target is  $\approx 26$  MeV, thus leaving a  $\approx 15$ -MeV discrepancy which we address next.

It is believed that three collective degrees of freedom ( $Q_{20}$ ,  $Q_{30}$ ,  $Q_{40}$ ), if not four (triaxial mode), are the barest minimum needed to describe the collective dynamics of fission. If so, one could expect that part of the available energy in the descent from saddle to scission would be transferred to two or three modes transverse to the fission direction. This possibility was studied previously [17] with two degrees of freedom ( $Q_{20}$ ,  $Q_{40}$ ). That work showed that  $\sim 2$  MeV are already taken by one transverse mode. With two other degrees of freedom a total of 4 or 5 MeV

could be taken up in these collective modes, at the expense of the fragment kinetic energy. Finally an other source of dissipation can result from the coupling of the collective dynamic with internal excitations [18]. A derivation of such coupling can be obtained in the framework of a generalization of the generator coordinate method including two quasiparticle excitations [19]. These degrees of freedom provide the means to dissipate part of the available 25 MeV from saddle to scission, without invoking statistical-mechanics arguments for low-energy fission.

Let us therefore consider different damping scenarios. Suppose that the 25 MeV potential energy liberated in the fission of  $^{240}\text{Pu}$  is shared in a 50/50 split between pre-scission fragment kinetic and excitation energies, then our prediction (TKE = 182.5 MeV and TXE = 24 MeV) precisely matches the experimental values. Even if we take a more conservative 25/75 distribution, one way or the other, the scenario we propose is still in good agreement with observations. It is rather striking that, without adjustable parameters, we obtain numbers that are simultaneously consistent with experiment for both the kinetic and excitation energies in this case. Although the results in this letter concern the most likely scission configuration, preliminary calculations of the kinetic energy for  $^{240}\text{Pu}$  for a wide range of scission configurations (symmetric to very asymmetric) are already showing a similar agreement with experiment.

Finally, let us mention that the concept of localization could have interesting applications as we approach the scission point. In effect, as we recognize pre-fragments, the values of the global constraints split into the contributions from those pre-fragments. Accordingly, we expect that the correct description of the system will rely on separate collective coordinates for those individual fragments. Although it remains to be verified, we believe that the localization of Fock space could provide a way to impose constraints separately on the pre-fragments, and thereby give a richer description of the fission mechanism.

This work was performed under the auspices of the US Department of Energy by the Lawrence Livermore National Laboratory under Contract DE-AC52-07NA27344.

- 
- [1] K.-H. Schmidt and B. Jurado, *Phys. Rev. Lett.* *104*, 212501 (2010).
  - [2] S. L. Whetstone Jr., *Phys. Rev.* *114*, 581 (1959).
  - [3] J. R. Nix, *Nucl. Phys.* *A130*, 241 (1969).
  - [4] K. T. R. Davies, R. A. Managan, J. R. Nix, A. J. Sierk, *Phys. Rev. C* *16*, 1890 (1977).
  - [5] W. Nörenberg, *Phys. Rev. C* *5*, 2020 (1972).
  - [6] L. Bonneau, P. Quentin, and I. N. Mikhailov, *Phys. Rev. C* *75*, 064313 (2007).
  - [7] H. Goutte, J. F. Berger, P. Casoli, and D. Gogny, *Phys. Rev. C* *71*, 024316 (2005).
  - [8] N. Dubray, H. Goutte, and J.-P. Delaroche, *Phys. Rev. C* *77*, 014310 (2008).
  - [9] J. Lennard-Jones, *Proc. Roy. Soc. A* *198*, 14 (1949).
  - [10] W. Younes and D. Gogny, *Phys. Rev. C* *80*, 054313 (2009).
  - [11] W. Younes and D. Gogny, in *Proceedings of the Fourth International Workshop on Nuclear Fission and Fission Product Spectroscopy*, Cadarache, France 2009 (American Institute of Physics, New York, 2009), p. 3.
  - [12] J.-F. Berger and D. Gogny, *Nucl. Phys.* *A333*, 302 (1980).
  - [13] C. Wagemans, E. Allaert, A. Deruytter, R. Barthélémy, and P. Schillebeeckx, *Phys. Rev. C* *30*, 218 (1984).
  - [14] K. Nishio, Y. Nakagome, I. Kanno, and I. Kimura, *J. Nucl. Sci. Tech.* *32*, 404 (1995).
  - [15] C. Tsuchiya, Y. Nakagome, H. Yamana, H. Moriyama, K. Nishio, I. Kanno, K. Shin, and I. Kimura, *J. Nucl. Sci. Tech.* *37*, 941 (2000).
  - [16] D. G. Madland, *Nucl. Phys.* *A772*, 113 (2006).
  - [17] J.-F. Berger, M. Girod, D. Gogny, *Nucl. Phys.* *A502*, 85 (1989).
  - [18] E. Moya de Guerra and F. Villars, *Nucl. Phys.* *A285*, 297 (1977).
  - [19] R. Bernard, H. Goutte, D. Gogny, and W. Younes, submitted to *Phys. Rev. C* (2011).

## Figures

Figure 1: (Color online). Interaction energies plotted as a function of neck size ( $Q_N$ ). The solid black and red dashed curves are the nuclear interaction energies before and after localization respectively (energy scale on left y axis), and the dotted green curve is the exchange part of the 2-body component of the interaction energy (energy scale on right y axis). The inset shows the effect of the localization on the densities of the fragments at scission.

Figure 2: (Color online) individual quasiparticle states before (top panel) and after (bottom panel) localization at scission. Proton states are shown as red crosses, and neutron states as black disks. The x axis gives the occupation ( $v_i^2$ ) of the state, while the y axis gives its localization ( $\ell_i$ ).

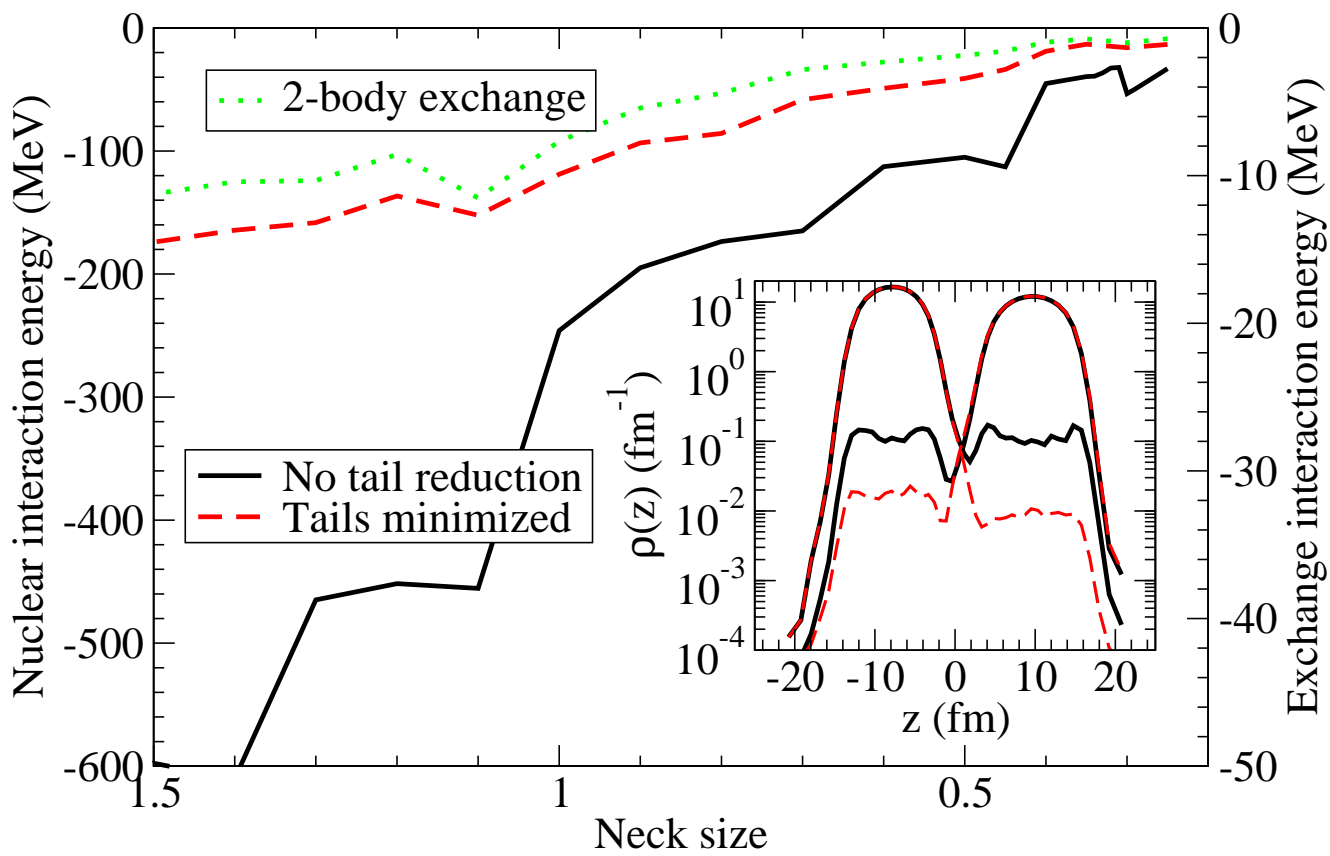


Figure 1

LC13266

08Jul2011

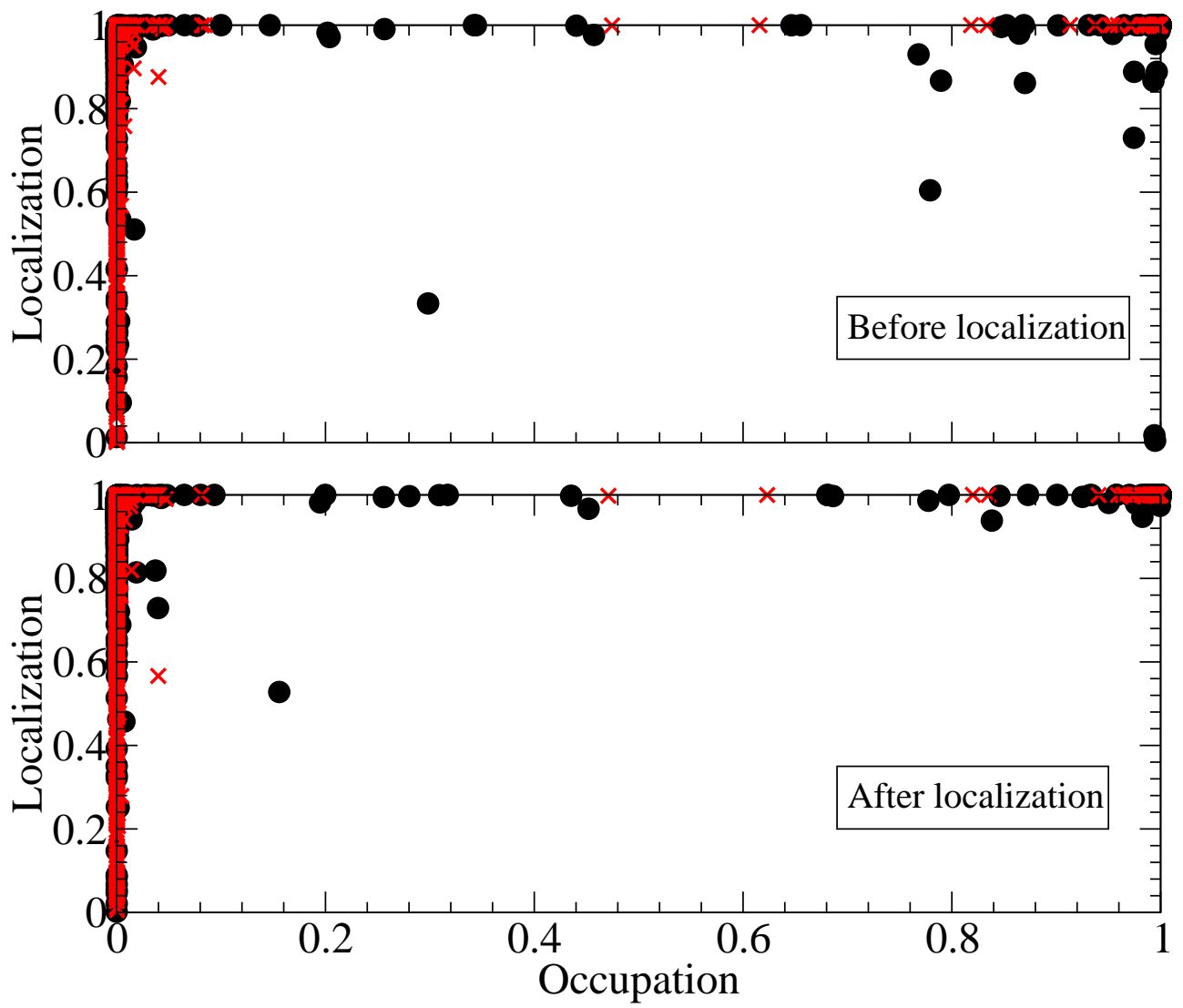


Figure 2 LC13266 08Jul2011